JOURNAL OF VIROLOGY, Mar. 1997, p. 2371-2382 Vol. 71, No. 3
0022-538X/97/$04.00+0

Characterization of the Components and Activity of Sonchus Yellow Net Rhabdovirus Polymerase

JOHN D. O. WAGNER† AND ANDREW O. JACKSON*

Department of Plant and Microbial Biology, University of California, Berkeley, California 94720

Received 2 August 1996/Accepted 9 December 1996

Sonchus yellow net virus (SYNV) is the best-characterized member of a group of plant rhabdoviruses that replicate in the host cell nucleus. Using a recently developed method for partial purification of active SYNV polymerase by salt extraction of nuclei from infected plant tissue (J. D. O. Wagner et al, J. Virol. 70:468–477, 1996), we have identified the nucleocapsid (N), M2, and L proteins as polymerase complex components (based on copurification with the polymerase activity and by coimmunoprecipitation assays). Furthermore, the L protein was shown by antibody inhibition analysis to be a functional component of the polymerase. A second complex of M2 and L proteins, thought to be a precursor to the polymerase complex, was also identified. In addition, we conducted a detailed characterization of SYNV RNA synthesis in vitro. The results demonstrate that the RNAs are transcribed sequentially, beginning with the N mRNA and followed successively by the remaining five mRNAs in the order of their genome organization. Gene expression conforms to a cascade pattern, with synthesis of the 3′-proximal N mRNA occurring at the highest level, followed by consecutively lower levels of transcription from each subsequent gene. The reaction conditions favor transcription over minus-sense RNA replication, which, we posit, is inhibited near specific signal sequences located on the antigenomic template. The results support the concept that the mechanism of transcription is highly conserved among diverse rhabdoviruses and are compatible with a unified model for the regulation of genomic and antigenomic RNA synthesis.

The rhabdoviruses comprise a large group of nonsegmented, negative-stranded RNA viruses that infect a broad array of eukaryotic hosts (57, 59). Many of these viruses infect organisms from different kingdoms (for example, plants and insects), and the viral infection can be localized in several distinct subcellular sites, including the cytoplasm and nucleus (27, 57, 59). Similarities in viral morphology and genome organization among these viruses suggest a general conservation between viruses, implying an infection strategy that is broadly applicable to diverse host species. However, the primary RNA sequence conservation is relatively low between the putative homologous genes of these viruses, perhaps suggesting specific adaptation to each particular milieu (7, 52). To date, most functional studies of rhabdovirus gene products have been conducted with the animal-infecting vesicular stomatitis virus (VSV) and rabies virus (4, 5, 14, 56). Sonchus yellow net virus (SYNV), the most thoroughly defined plant rhabdovirus, appears to be only distantly related to VSV and rabies virus and differs both in host specificity (plants and aphid vector) and the subcellular site of replication (nucleus versus cytoplasm) from these viruses (8, 27, 51, 58). However, SYNV and Borna disease virus, which belongs to a distinct family of negative-strand viruses, are similar in that both are replicated in nuclei (50). Thus, studies of SYNV provide an excellent opportunity to define conserved and divergent functions within the nonsegmented RNA virus families.

SYNV infects composite and solanaceous plant species (for a review, see reference 27). The 13,720-nucleotide (nt) SYNV genome encodes six proteins, all of which are found in the purified virion (20, 28, 51, 54). These include (from 3′ to 5′ on the genome) a nucleocapsid protein (N; 475 amino acids), a putative phosphoprotein (M2; 345 amino acids), a protein of unknown function (sc4; 324 amino acids), a putative matrix protein (M1; 286 amino acids), a glycoprotein (G; 632 amino acids), and a putative polymerase protein (L; 2,116 amino acids) (Fig. 1) (see reference 51 and references therein). Little direct evidence exists for the function of the individual proteins during infection.

Biochemical fractionation of the VSV virion-associated polymerase complex, as well as more recent studies using viral proteins expressed in HeLa cells with vaccinia virus vectors and T7 polymerase, have demonstrated that the VSV N, phosphoprotein (P), and L proteins are essential for transcription and replication of viral RNA (16, 25, 38, 39, 41, 42). Similarly, it has been shown recently that the rabies virus polymerase requires the N, M1, and L proteins, the homologs of the VSV N, P, and L proteins (10, 11). For the VSV, the L protein is believed to be the core component of the polymerase (12, 37). The N protein encapsidates the genomic and antigenomic RNAs and is an obligate constituent of the template for the polymerase. The N protein also has a role in the transition between transcription and replication during the infection cycle and appears to have additional functions during transcription (6, 15, 41, 46). Although the role of the P protein is still unclear, it probably mediates the interactions between the N protein and the template RNA (25, 33, 44), and it may have a function in RNA elongation (12, 13).

SYNV gene expression occurs through transcription of the genomic RNA into discrete mRNAs that are polyadenylated and are selectively partitioned to free and membrane-bound polysomes in the cytoplasm (35, 36). In infected cells, the L mRNA is present at a lower abundance than the 3′-encoded mRNAs, suggesting that relative mRNA abundance could be an important component of the regulation of gene expression (29, 47). Furthermore, the minus-sense genomic RNA is detected later than the SYNV mRNAs in protoplasts, suggesting that the processes of transcription and replication are tempo-

* Corresponding author. Phone: (510) 642-3906. Fax: (510) 642-9017.

† Present address: Division of Biology 147-75, California Institute of Technology, Pasadena, Calif.

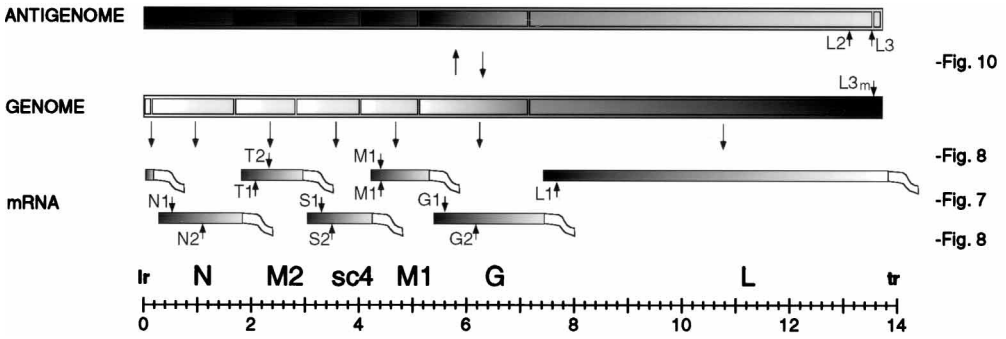

FIG. 1. Relative locations within the SYNV genome of the oligonucleotide probes used for analysis of the SYNV polymerase products. The antigenomic, genomic, and messenger RNAs are depicted to scale, shaded from 5′ (black) to 3′ (white) ends. Viral replication or transcription is indicated by arrows from templates to products. Locations of each viral gene, as well as the plus-strand leader (lr) and trailer (tr) sequences, are illustrated at the bottom. The predicted sites of hybridization of individual DNA oligonucleotides, and therefore the RNase H-mediated cleavage sites, are indicated by arrows above or below the appropriate target RNAs. Figure designations on the right indicate the figures showing the cleavage data for each set of oligonucleotide probes. The scale bar at the bottom provides a nucleotide reference.

rally regulated (29). However, the mechanisms underlying potential regulation of gene expression and viral replication are unknown.

VSV transcription has been shown to be sequential, in that the synthesis of each viral mRNA is dependent on the prior synthesis of the mRNA located immediately upstream on the viral genome (1, 3). In addition, the relative rates of synthesis of the individual mRNAs in vitro are regulated in a cascade pattern, with the rate of synthesis of the five mRNAs reflecting the location of each viral gene on the genome (3′ to 5′) (26). Since the comparative accumulation of the VSV mRNAs and their encoded proteins resembles the relative rates of mRNA transcription, and no appreciable differences in the rates of degradation of the individual mRNAs are observed in vivo, it is likely that the expression of VSV genes is regulated primarily at the level of transcription (45, 48, 53). Replication, unlike transcription, requires a pool of N protein to encapsidate the nascent plus-sense antigenomic RNAs and the minus-sense genomic RNAs (41). Thus, although similar polymerase complexes are involved in mRNA transcription and replication of the two genome-length RNAs, replication is maintained only under conditions that favor nascent RNA encapsidation.

We have recently developed a procedure for partial purification of SYNV polymerase from the nuclei of infected tobacco leaf tissue (54). In the initial study, we demonstrated that the polymerase extract is able to synthesize polyadenylated plus-strand leader RNA and full-length N and M2 mRNAs during the incubations for up to 1 h. In the present study, by further purification, we show that the L, N, and M2 proteins are physically associated with the polymerase activity. Furthermore, the results show that upon longer incubations (for up to 8 h), the polymerase functions primarily as a transcriptase, because the major products are polyadenylated, full-length mRNAs that can be translated into viral proteins. Kinetic analyses also suggest that SYNV transcription, like that of VSV, is sequential and that the accumulation of the mRNA products follows a cascade pattern of N > M2 > sc4 > M1 > G > L. Finally, we show that initiation of viral replication occurs in the polymerase extract, while synthesis of large genome-sense RNAs is not apparent. These results suggest that the processes of transcription and replication are functionally distinct and that replication in vitro is inhibited at the level of elongation. Overall, the results suggest that mechanistic similarities between SYNV and VSV RNA synthesis have been conserved during the evolution of these plant and animal viruses.

MATERIALS AND METHODS

Virus culture and polymerase extracts. SYNV (ATC PV-263) was maintained in a greenhouse under ambient conditions by serial passages in *Nicotiana edwardsonii*, a hybrid tobacco (9). Tissue was harvested at 10 to 14 days after inoculation and stored as described previously (54). Polymerase extracts were prepared by isolation of nuclei from frozen leaf tissue, using Percoll gradients followed by extraction of the nuclei in 100 mM $(NH_4)_2SO_4$ (54).

Sucrose gradient analysis of the SYNV polymerase extract. Prior to centrifugation, the polymerase extract was diluted with an equal volume of buffer [50 mM $(NH_4)_2SO_4$, 25 mM HEPES (pH 8.0), 5 mM $MgCl_2$, 3 mM dithiothreitol (DTT)] to reduce the glycerol concentration. The diluted sample was layered on a 3.6-ml linear sucrose gradient [5 to 25% sucrose prepared in 20% glycerol–50 mM $(NH_4)_2SO_4$–25 mM HEPES (pH 8.0)–5 mM $MgCl_2$–3 mM DTT] followed by centrifugation at 4°C for 30 min at 50,000 rpm (177,000 × *g*) in an SW60Ti rotor (Beckman Instruments, Palo Alto, Calif.). The conditions of in vitro transcription reactions and slot blot hybridization were as described previously (54) except that all of the RNA from each gradient fraction was hybridized to a single slot blot. Sodium dodecyl sulfate (SDS)-polyacrylamide gel electrophoresis (PAGE) was conducted with a 25-μl aliquot of each gradient fraction in discontinuous gels (10% polyacrylamide in the separation gel), using standard procedures (19). The proteins in the gel were transferred to nitrocellulose and analyzed with anti-L (α-L) antiserum, horseradish peroxidase-conjugated secondary antibody (Bio-Rad), and the Amersham ECL system or with α-SYNV antiserum, alkaline phosphatase-conjugated secondary antibody, and bromochloroindolyl phosphate-nitroblue tetrazolium (54).

Preparation and analysis of protoplast extracts. Protoplasts were prepared from *Nicotiana benthamiana* plants, and batches of 3×10^6 were transfected with purified SYNV by using polyethylene glycol (29). At 22 h posttransfection, the protoplast incubation medium volume was decreased fivefold and [^{35}S]methionine was added. For preparation of native protoplast extracts, the protoplasts were resuspended in disruption buffer (10 mM HEPES [pH 8.0], 5 mM $MgCl_2$, 4 mM KCl, 1 mM β-mercaptoethanol, 1 mM phenylmethyl sulfonyl fluoride, 0.5 μg of leupeptin per ml, 1 μg of pepstatin per ml, 1 μg of aprotinin per ml), incubated for 10 min, and then disrupted by passing 10 times through a 26-gauge needle. The buffer was adjusted to 100 mM $(NH_4)_2SO_4$, and the samples were incubated with rocking for 10 min to extract viral complexes from the nuclei. Following extraction, the supernatant obtained by centrifugation for 10 min at 14,000 rpm in a microcentrifuge was used directly for immunoprecipitation or gradient centrifugation. For the detergent-treated controls, extracts were prepared by protoplast lysis in disruption buffer amended with 1% SDS followed by passage through a 26-gauge needle. The extract was subsequently boiled for 3 min, and a supernatant fraction was obtained after centrifugation for 10 min at 14,000 rpm in a microcentrifuge.

Immunoprecipitations were carried out by using standard procedures at 4°C in 500-μl reaction mixtures containing 200 μl of native protoplast extract or 50 μl of SDS protoplast extract diluted with immunoprecipitation buffer (2% [wt/vol] bovine serum albumin, 100 mM NaCl, 50 mM Tris [pH 8.0], 0.1% [vol/vol] Nonidet P-40 [omitted in SDS protoplast extract immunoprecipitations], protease inhibitors [1 mM phenylmethyl sulfonyl fluoride, 0.5 μg of leupeptin per ml, 1 μg of pepstatin per ml, and 1 μg of aprotinin per ml]) (19). The samples were precleared by incubation with preimmune sera corresponding to the α-N and α-M2 antibodies and protein A-Sepharose beads (Pharmacia) prior to immunoprecipitation (19).

In vitro reactions and RNA analysis. Polymerase reactions were normally conducted at 28°C in a total volume of 200 μl containing 20 μl of polymerase extract in 6 mM $MgCl_2$–50 mM $(NH_4)_2SO_4$–12.5 mM HEPES (pH 8.0)–2 mM

DTT–1 mM ATP–0.5 mM CTP–0.5 mM GTP–20 μM unlabeled UTP–50 μCi [α-^{32}P]UTP–20 U of DNase I per ml–200 U of RNasin (Promega, Madison, Wis.) per ml–2% (vol/vol) glycerol. Deviations from these conditions are noted for specific experiments. RNA products were purified as described previously (54). For agarose gel analysis, RNA was denatured by glyoxylation in 70% (vol/vol) formamide at 55°C, electrophoresed through 1% agarose in TAE buffer (40 mM Tris-acetate, 1 mM EDTA) at 100 V, and fixed in 100% methanol (54). Oligonucleotide-mediated RNase H cleavage was conducted prior to gel electrophoresis for 30 min at 37°C with 1 μg of each oligonucleotide and 0.5 U of RNase H in 50 mM Tris (pH 8.3)–10 mM DTT–60 mM NaCl–1.5 mM $MgCl_2$ (30). Gel electrophoresis results were obtained from PhosphorImager (Molecular Dynamics, Sunnyvale, Calif.) exposures and were processed with Adobe Photoshop (Adobe Systems, Mountain View, Calif.) without alteration except for the order of the lanes.

cDNA and oligonucleotide probes. The genomic locations of all SYNV-specific probes used in this study are shown in Fig. 1. The genome-sense oligonucleotides used and their nucleotide positions with respect to SYNV genome (GenBank accession number L32603) are as follows: N1, 415 to 398; N2, 1068 to 1049; T1, 1945 to 1925; T2, 2297 to 2281; S1, 3110 to 3092; S2, 3442 to 3426; M1, 4299 to 4281; G1, 5362 to 5344; G2, 6111 to 6093; L1, 7417 to 7399; L2, 13325 to 13306); and L3, 13547 to 13525. The antigenome-sense oligonucleotides are N2m (725 to 746) and L3m (13547 to 13525).

RESULTS

SYNV polymerase activity copurifies with a complex containing the N, M2, and L proteins. Following disruption with detergent and salt, the ribonucleoprotein (RNP) core of the SYNV virion has previously been shown to migrate in sucrose rate zonal gradients at 200S to 250S (28). Recently, we have developed a procedure for partially purifying SYNV polymerase activity from infected plant tissue (54). If the SYNV transcription activity that we have detected in the polymerase extracts is associated with an RNP complex resembling the virion cores, it would be expected to sediment at a similar rate. Polymerase extracts were therefore separated on sucrose gradients, and individual fractions were assessed for RNA synthesis activity in vitro. SYNV RNA synthesis was detected by slot blot hybridization of radiolabeled products to two cDNA clones derived from the SYNV genome (in the leader-5′ N gene region and the M2 gene region), as described previously (54).

During centrifugation, all of the detectable SYNV-specific polymerase activity migrated into the gradient, demonstrating that the activity is associated with a rapidly sedimenting complex (Fig. 2A). The majority of the activity was found in the center of the gradient (fractions 4 and 5), displaying mobility in the gradient similar to that of the previously characterized SYNV-core RNP complex. In contrast, hybridization to the cloning vector lacking an SYNV-specific cDNA insert was low and was randomly distributed through the gradient (Fig. 2A, neg. cont.). Examination of the distribution of the SYNV proteins by immunoblotting revealed that the N, M2, and L proteins were most abundant in fractions 4 and 5, which contained the peak polymerase activity (compare Fig. 2A to C). Furthermore, the relative ratios of these three proteins in individual fractions were similar (except in the upper two fractions of the gradient), suggesting that they are components of a multisubunit complex. In contrast, the G and M1 proteins were concentrated near the top of the gradient, which contained only minor amounts of SYNV polymerase activity. The sc4 protein was not detected in any of the fractions in assays using an sc4-specific antibody (51). Thus, these results suggest that the SYNV transcriptase activity is associated with a specific complex containing the viral RNA template and the N, M2, and L proteins.

Immunoprecipitation of extracts from protoplasts reveals two distinct SYNV protein complexes. As an alternative strategy to characterize the protein components of the SYNV polymerase complex, we next analyzed radiolabeled proteins from protoplast extracts by immunoprecipitation. A new protocol was developed for disruption of SYNV-infected protoplasts to yield an extract which was likely to contain intact SYNV transcription-replication complexes. The protocol included mechanical disruption and incubation in 100 mM $(NH_4)_2SO_4$, to

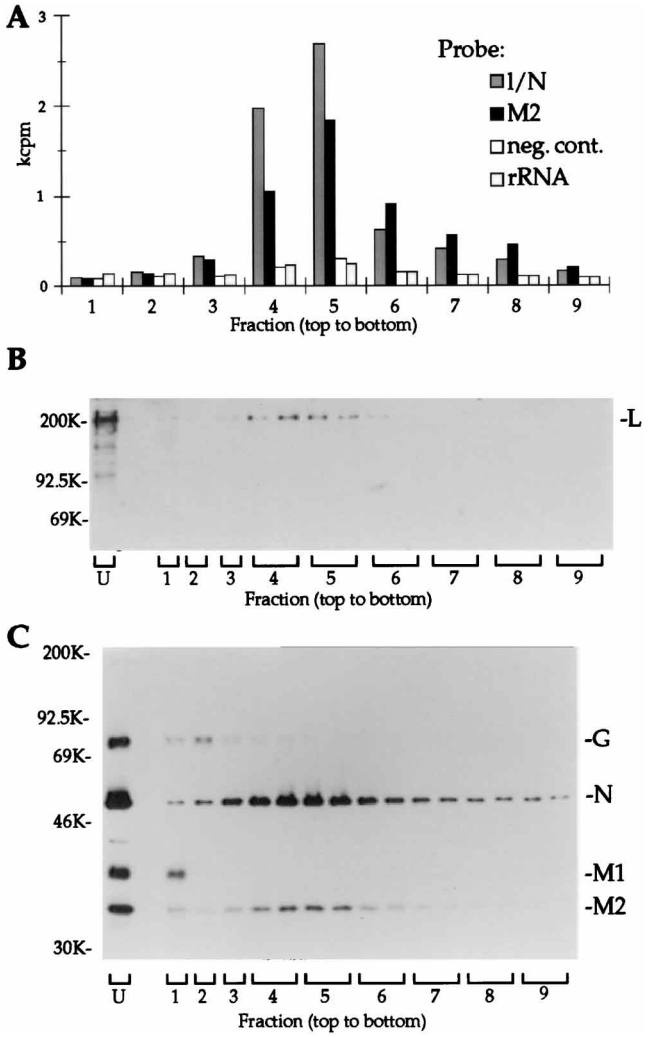

FIG. 2. Analysis of SYNV polymerase extract following separation by sucrose gradient centrifugation. The gradient was fractionated into 18 200-μl portions. For the transcriptase activity assay shown in panel A, the 18 gradient fractions were pooled pairwise to yield nine 400-μL assay fractions. However, in the Western blot analyses depicted in panels B and C, only the top two pairs of gradient fractions were pooled. (A) In vitro transcription activity in sucrose gradient fractions. An aliquot (50 μl) of each of the nine pooled assay fractions was incubated for 30 min in a 200-μl RNA polymerase reaction, and the in vitro-radiolabeled RNA was analyzed by slot blot hybridization. Radiolabeled RNA hybridized to the SYNV-specific cDNA probes corresponding to the plus-strand leader and the first 118 nt of the N gene (▧, pJW2) and the entire M2 gene (■, p3ZT1), a nonspecific negative control, pBSKS+ II (□, neg. cont.), and the rRNA-specific pRS1 plasmid (▨, rRNA) was quantified and plotted for each fraction. Plasmids pJW2, p3ZT1, and pRS1 have been described elsewhere (54). The probe pBSKS+ II is the cloning vector DNA lacking a cDNA insert. (B) Western blot analysis of the SYNV L protein in the sucrose gradient fractions, using an L-specific antiserum (54). The fraction numbering indicated by brackets corresponds to that shown in panel A. An unfractionated nuclear extract (lane U, 12.5 μl) was included on the gel for comparison. The locations of molecular weight markers on the gel are shown on the left, and the position of the L protein is indicated on the right. (C) Western blot localization of the SYNV G, N, M2, and M1 proteins (shown on the right) in the sucrose gradient fractions, using α-SYNV antiserum. Lane designations are as in panel B.

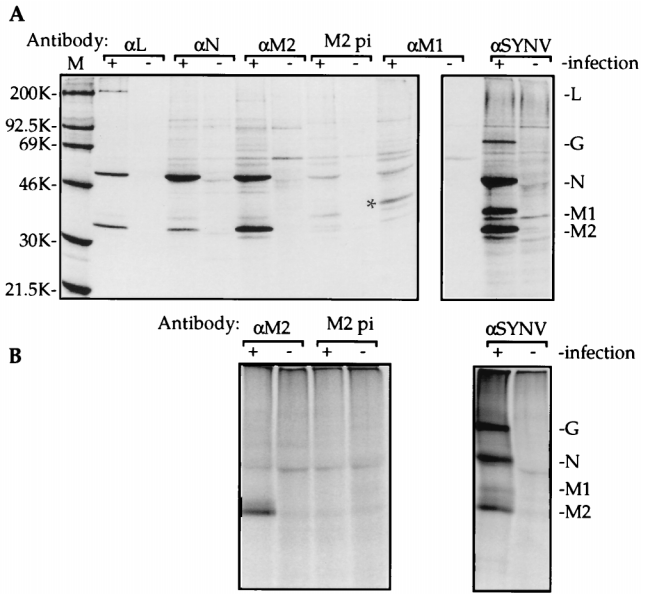

FIG. 3. Coimmunoprecipitation of SYNV proteins from extracts of SYNV-infected protoplasts with SYNV-specific antisera. Extracts were prepared from SYNV-infected and mock-infected tobacco leaf protoplasts radiolabeled in vivo (0.5 mCi of [^{35}S]methionine/10^6 protoplasts) by disruption in the absence (A) or presence (B) of 1% SDS, where the sample was also boiled for 3 min prior to centrifugation. Aliquots of each extract were precleared with α-SYNV preimmune serum collected prior to immunization with SYNV (28). The aliquots were incubated with antiserum raised against the SYNV L (lanes αL), SYNV N (lanes αN), SYNV M2 (Lanes αM2), or SYNV M1 (lanes αM1) protein or against SDS-disrupted SYNV virions (lanes αSYNV) or with preimmune serum (lanes M2 pi) that was collected before immunization with the M2 antibody. Precipitates from SYNV-infected protoplast extracts are labeled with a + and those from mock-infected protoplasts are labeled with a − above the respective lanes. Proteins and protein complexes were immunoprecipitated with protein A-Sepharose beads and visualized following separation by SDS-PAGE. The locations of specific SYNV proteins are shown to the right of panels A and B, and the positions of the molecular weight markers are shown to the left of panel A. Note that the samples in panel A were run on two separate gels (as identified by the boxes) and that the M1 protein in the α-M1 immunoprecipitate (identified by an asterisk) migrates slightly above M1 in the α-SYNV immunoprecipitate. This is an artifact due to aberrant electrophoresis of this sample caused by its location at the edge of the gel.

mimic the procedure used for isolation of polymerase activity from whole leaves (54).

Immunoprecipitation of the $(NH_4)_2SO_4$ supernatant with the α-SYNV antibody revealed that the protoplast extract contained significant quantities of radiolabeled N, M2, M1, and G proteins (Fig. 3A, lane αSYNV +), and immunoprecipitation with the α-L antibody resulted in recovery of a radiolabeled protein corresponding in size to the L protein, as was expected. Furthermore, polypeptides of electrophoretic mobility corresponding to the N and M2 proteins were coprecipitated with the α-L antibodies (Lane αL +). The α-N and α-M2 antisera specifically precipitated both proteins (Fig. 3A, lanes αN + and αM2 +). Immunoprecipitation of M1 with the α-M1 antiserum was relatively inefficient (Fig. 3A, lane αM1 +); the putative M1 protein is identified by an asterisk. However, more importantly, coprecipitation of other viral proteins, particularly the N, M2, and L proteins, was not apparent.

In all cases, the antibody-mediated precipitation was specific for the appropriate antigen. Immunoprecipitation of polypeptides which comigrated with the SYNV proteins on SDS-polyacrylamide gels was not detected from mock-infected protoplasts with any of the antibodies used in the assay (Fig 3A, lanes −). In addition, only trace amounts of SYNV N and M2 proteins and several nonviral polypeptides were precipitated in control reactions performed with preimmune serum to the α-N and α-M2 antibodies (data not shown and Fig. 3A, lane M2 pi +). The low levels of proteins detected in pellets obtained with the preimmune sera were probably nonspecific aggregates, as further substantiated by the absence of precipitated SYNV proteins following boiling of the sample (Fig. 3B, lane M2 pi +).

To provide evidence that coprecipitation of viral proteins was due to interactions between the coprecipitated proteins, rather than nonspecific direct interactions of the noncognate proteins with the antibodies, protoplast extracts were boiled in 1% SDS prior to immunoprecipitation with α-SYNV, α-M2, or the M2 preimmune serum. Under these conditions, the immunoprecipitate obtained with α-M2 contained M2 protein but was free of detectable N protein (Fig. 3B, lane αM2 +). The precipitate obtained with the α-SYNV antiserum was similar in profile to that obtained following precipitation without prior SDS and boiling treatment and contained substantial quantities of N protein as well as the M2, M1, and G proteins (Fig. 3B, lane αSYNV +; compare with Fig. 3A, lane αSYNV +). Thus, the boiling treatment had little effect on the direct antibody-antigen interactions observed with this serum or on the integrity of the N protein. Therefore, these results strongly suggest that the observed α-M2 immunoprecipitation of the N protein from the unboiled sample was indirect and most likely was mediated by binding of antibodies to M2 complexes containing the N protein. Thus, these data indicate direct or indirect physical association of L with N and M2 and of M2 with N in complexes present in the protoplast extract.

The results of the gradient fractionation experiments presented in Fig. 2 suggested that the L, N, and M2 proteins were each components of a large complex that was responsible for viral transcription activity in vitro. Since the immunoprecipitation of the radiolabeled proteins was conducted with unfractionated extracts, it was unclear whether coprecipitation of the N and M2 proteins by α-L was due to immunoprecipitation of this putative SYNV polymerase complex (Fig. 2) or whether alternative complexes of L with N or M2 were immunoprecipitated. To distinguish between these possibilities, we fractionated the in vivo-labeled protoplast extract over a sucrose gradient prior to immunoprecipitation. Results with the α-SYNV antiserum revealed large amounts of the N, M2, and M1 proteins in the upper regions of the gradient (Fig.4A, fractions 1 and 2). Furthermore, substantial concentrations of the N and M2 proteins, but not M1, were present in a second peak in the middle region of the gradient (fractions 4 and 5). Portions of the sucrose gradient fractions were also analyzed for SYNV-specific polymerase activity (Fig. 5A). SYNV transcriptase activity was detected through accumulation of RNAs corresponding in size to SYNV N and M2 mRNAs as described previously (54). Quantification of these RNAs revealed that the majority of the SYNV transcriptase activity was localized in fractions 4 and 5 of the gradient (Fig. 5A), with an overall profile that was very similar to that of the polymerase extract from infected plants (compare with Fig. 2A). The RNA synthesis activity corresponded exactly with the apparent N- and M2-containing complexes detected with the α-SYNV antiserum (fractions 4 and 5).

Physical association of the viral proteins in fractions obtained from sucrose gradient centrifugation was probed by immunoprecipitation with the α-L and α-M2 antisera. Each serum immunoprecipitated a complex from the middle fractions of the gradient that contains at least the SYNV N and M2 proteins (Fig. 4B and C). Presumably due to the low abundance of L in the complex, only trace amounts of the L protein were detected in precipitates from fractions 4 and 5, using

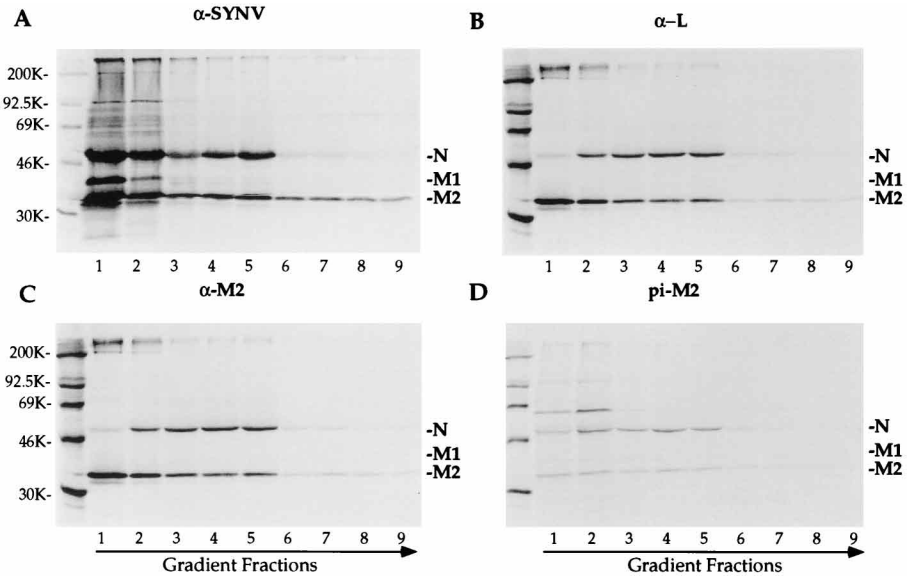

FIG. 4. Immunoprecipitation of SYNV-specific complexes separated by sucrose gradient fractionation of extracts recovered from infected protoplasts. SYNV-infected leaf protoplasts were labeled in vivo with [^{35}S]methionine (1 mCi/10^6 protoplasts), disrupted in disruption buffer, and eluted with 100 mM $(NH_4)_2SO_4$. Microcentrifuged extracts were fractionated on a sucrose gradient as for Fig. 2. Portions (100 μl) of each gradient fraction were immunoprecipitated with α-SYNV (A), α-L (B), or α-M2 antiserum (C) or with the α-M2 preimmune serum (pi-M2; D) and then visualized following separation of the immunoprecipitate in SDS-gels. The individual gradient fractions are shown in lanes 1 to 9, with the direction of sedimentation indicated by an arrow below each panel. The locations of the SYNV proteins are shown on the right, and those of the molecular weight markers are shown on the left.

either the α-L or α-M2 antiserum, when the darker exposures were examined (data not shown). However, compelling, albeit indirect, evidence that the L protein was also a component of the complex is provided by the fact that α-L coprecipitated the other viral proteins from these fractions. Only minor amounts of N and M2 proteins were precipitated by the M2 preimmune serum, demonstrating the specific nature of the precipitation observed with α-L and α-M2 sera (Fig. 4D).

Quantification of the N protein coprecipitated from fractions of the gradient-separated protoplast extract by the α-L or α-M2 antibody revealed that the N protein profile corresponds closely with that of transcription activity (compare Fig. 5A and B). In sharp contrast, immunoprecipitation of the N protein with the α-SYNV antibody (Fig. 4A) revealed that the majority of the precipitated N protein was localized in fractions 1 and 2 of the gradient. Similar trends were observed in three experiments, including one in which a longer centrifugation was conducted. In this case, the maximal transcriptase activity and the α-L-precipitable protein complex sedimented deeper in the gradient than in Fig. 5 (data not shown). Two conclusions follow from these results: first, the N protein is part of a complex that corresponds to the active SYNV polymerase complex in its sedimentation pattern; and second, the M2 and L proteins are physically associated with the complex, since it was precipitated by M2- and L-specific antibodies. Thus, the results with the protoplast extracts corroborate the data obtained with the polymerase extracts from the nuclei of infected plants (Fig. 2).

The amount of the M2 protein present in the α-L and α-M2 immunoprecipitates of the gradient fractions was also quantified (Fig. 5C). The profile of immunoprecipitated M2 differed sharply from that of the transcription activity (Fig. 5A) and that of the coprecipitated N protein (Fig. 5B), suggesting that the α-L and α-M2 antibodies might have bound to M2 complexes that were distinct from the polymerase complex. Highly specific coprecipitation of the M2 and L proteins from fractions 1 and 2 of the gradient by the α-L antiserum also indicates that specific M2-L complexes were present in the extract. Therefore, it is likely that the M2 protein associates with the L protein in vivo to form a slowly sedimenting complex. Since α-L coprecipitates little or no N protein from the upper gradient fractions (Fig. 5B; compare the N precipitated by α-L with that precipitated by the M2 preimmune serum), the data suggest that the N protein is not a component of the L-M2 complex.

The SYNV polymerase activity is inhibited by L protein-specific antibodies. The immunoprecipitation results revealed that N, M2, and L protein-specific antisera each bind to a native complex whose sucrose gradient fractionation pattern correlated with that of the SYNV transcription activity (Fig. 5B and data not shown). To assess whether the binding of these antibodies to the complex had a discernible effect on in vitro transcription, we incubated the polymerase extract in buffer alone or with α-L, α-N, α-M2, or preimmune antiserum and then conducted in vitro RNA synthesis assays. SYNV-specific mRNAs were identified by characteristic mobility following agarose gel electrophoresis of the RNA products. In a representative experiment, addition of the α-L antibody to the polymerase extract led to a dramatic reduction (>90%) of the polymerase activity detected in the preimmune antibody control (Fig. 6; compare lanes 1 and 4). Similar results were obtained in each of three independent experiments. In contrast, after addition of α-N or α-M2 antiserum, the polymerase activity detected was similar to that in the control, suggesting that these antibodies did not inhibit the polymerase activity (Fig. 6; compare lanes 2 to 4).

Sequential synthesis of SYNV mRNAs occurs in vitro. To investigate the kinetics of SYNV transcription in polymerase extracts, the radiolabeled RNA products synthesized in vitro during various 1-h time periods (0 to 1, 1 to 2, 3 to 4, and 7 to 8 h) were recovered. We have shown that RNase H cleavage mediated by DNA oligonucleotides that hybridize to specific regions of the radiolabeled transcripts is a simple and effective means for identification of individual SYNV RNA species

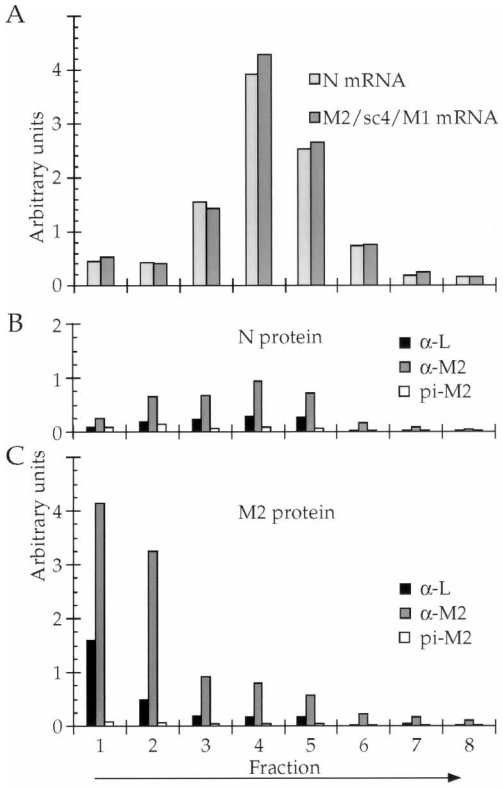

FIG. 5. Quantification of SYNV transcription and N and M2 protein immunoprecipitation from sucrose density gradient fractions of native protoplast extracts following labeling in vivo with [^{35}S]methionine. (A) Extracts from infected protoplasts (unlabeled) were prepared and fractionated as for Fig. 4. Aliquots of the upper eight fractions obtained (50 μl) were included in RNA polymerase reactions in vitro (1 h, standard conditions except for the presence of sucrose from the gradient), the radiolabeled RNA was purified and separated by denaturing agarose electrophoresis, and the ^{32}P-labeled RNA that comigrated with the N (▤) and M2 (▨) mRNA markers on the gel was quantified in arbitrary units. (B and C) The N protein (B) and M2 protein (C) detected in the immunoprecipitates in the presence of the α-L (■) and α-M2 (▨) antisera and the M2 preimmune serum (pi-M2; □) from the individual gradient fractions of the experiment presented in Fig. 4 were quantified and plotted as a function of their location in the gradient. Note that in panels B and C, the ^{35}S units on the *y* axes are arbitrary but are directly comparable.

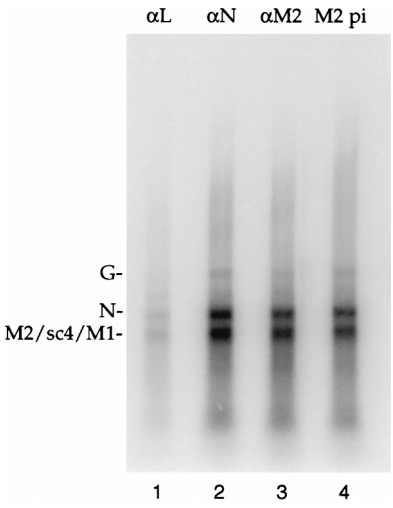

FIG. 6. Effects of the N, P, and L antibodies on transcription. The SYNV polymerase extract (20 μl) was incubated at 4°C for 1 h in 200 μl of transcription reaction mixtures lacking nucleotides in the presence of 20 μg of antiserum raised against the SYNV L (lane 1), N (lane 2), or M2 (lane 3) protein, or with the preimmune serum to the M2 antibody (M2 pi; lane 4) in transcription buffer. Transcription was initiated by addition of nucleotides and incubation for 2 h at 28°C. The transcription products were purified and visualized following gel electrophoresis. The locations of the specific SYNV mRNAs are shown on the left.

present in a heterogeneous population (54). Therefore, to measure the timing of transcriptional initiation of the six SYNV mRNAs, we synthesized a series of DNA oligonucleotides complementary to each mRNA (Fig. 1). Cleavage of the in vitro-labeled mRNA products was expected to generate a fragment of ~250 nt corresponding to the 5′ end of each mRNA that could be identified and quantified following PAGE. The sites of DNA oligonucleotide-RNA hybridization were selected such that GC contents were comparable between sites to ensure uniform melting temperatures and thereby minimize inconsistencies that might have resulted from differential hybridization kinetics.

Analysis of the total products radiolabeled in the first hour revealed that only the N gene mRNA accumulated in appreciable quantities (Fig. 7A). Between 1 and 2 h, radiolabeled products corresponding to the N, M2 and sc4 transcripts accumulated (Fig. 7B), and synthesis of the 5′ ends of all six SYNV mRNAs was detected between both 3 and 4 h and 7 and 8 h (Fig. 7C and D). Based on the published sequences, complete digestion of the mRNA in each RNA-DNA heteroduplex was expected to yield products of 249 nt (N), 253 nt (M2), 252 nt (sc4), 243 nt (M1), 233 nt (G), and 241 nt (L). The relative size of each digestion product, as resolved by gel electrophoresis, agrees well with the sizes of these predicted fragments (Fig. 7). Thus, the results suggest that the resolved products correspond to mRNA transcripts accurately initiated or processed at the 5′ end.

Three observations follow from the data presented in Fig. 7. First, levels of accumulation of the 5′ end of the N mRNA were similar during all of the 1-h periods. Thus, the apparent rate of transcription of this RNA was nearly constant, providing an internal reference for the transcription of the other viral genes. Second, after the initial detection of each specific product, labeling of that product was detected during all successive labeling periods, suggesting that multiple rounds of mRNA transcription were initiated in vitro. Third, except for the N-specific RNA, each product accumulated with a distinct, biphasic pattern, with an initial low to negligible level followed by easily detectable synthesis. Following the initial detection of each of these products, the amount detected in successive 1-h periods decreased gradually. These results suggest that the transcription of the mRNAs (except possibly the N mRNA) increases dramatically during the course of the experiment. The pattern of the observed increase in transcription was sequential, with products corresponding to the genes located near the 3′ end of the SYNV genome appearing earlier than those located further toward the 5′ end.

To quantitate relative transcription, the radioactivity incorporated into each RNA cleavage product in Fig. 7 was determined. The results were corrected by division by the number of uridine residues in the expected products and then expressed as a percentage of the quantity of N mRNA product measured at each time point (Table 1). This quantification reveals that mRNA synthesis was discontinuous, because different molar amounts of the individual products were synthesized in each of the 1-h periods examined (Table 1). Furthermore, an overall trend of decreasing levels of RNA production down the genome from the 3′-proximal N gene to the 5′-proximal L gene was apparent (Table 1). Thus, from these results, we conclude that both the timing and the accumulation of the 5′ end mRNA

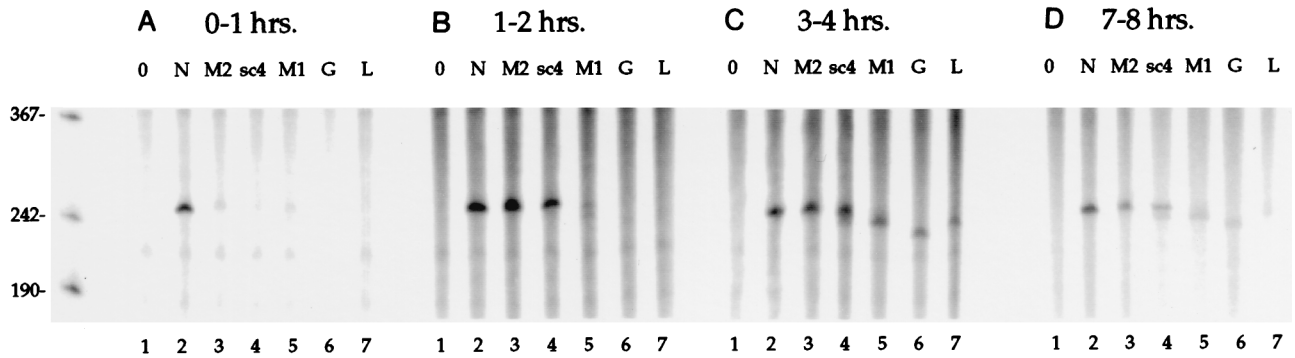

FIG. 7. RNase H analysis to define the kinetics of initiation of the SYNV transcription products. Duplicate reactions with the polymerase extract were conducted under standard conditions except that [α-^{32}P]UTP was added 1 h prior to termination. The labeling, in relation to initiation of the in vitro reactions, was conducted at 0 to 1 h (A), 1 to 2 h (B), 3 to 4 h (C), or 7 to 8 h (D). Aliquots of the unfractionated RNA recovered from each reaction were digested with RNase H without hybridization to a DNA oligonucleotide (lanes 1) or after hybridization to DNA oligonucleotides specific to SYNV mRNAs N (oligonucleotide N1; lanes 2), M2 (oligonucleotide T1; lanes 3), sc4 (oligonucleotide S1; lanes 4), M1 (oligonucleotide O1; lanes 5), G (oligonucleotide G1; lanes 6), and L (oligonucleotide L1, lanes 7). The specific digestion products were detected after separation by denaturing 6% polyacrylamide gel electrophoresis. The migration of radiolabeled single-stranded DNA markers on the gel is shown on the left in nucleotides.

products are consistent with a cascade pattern of transcription in vitro which is similar to that detected previously with VSV.

Full-length, polyadenylated SYNV mRNAs are transcribed. Measurements of the incorporation of nucleotides into the putative mRNA 5′-end fragments permit an estimation of the relative rates of transcriptional initiation of the viral genes. However, potentially disparate rates of attenuation or premature termination could have altered the levels of full-length mRNA synthesis. Therefore, we performed experiments to examine the accumulation of full-length, polyadenylated mRNAs in vitro. In these experiments, polyadenylated RNAs synthesized after various incubation periods in vitro were selected with oligo(dT)-cellulose. RNase H digestions were then carried out in separate reactions with oligonucleotides complementary to the first five SYNV mRNAs, and the products were resolved by denaturing agarose gel electrophoresis (Fig. 8). A specific assay for the L mRNA was omitted because products of the predicted size were not visible on the agarose gel (Fig. 8). RNase H digestions in the absence of SYNV-specific oligonucleotide revealed that three different sizes of radiolabeled RNA species predominated after 6 h of synthesis (Fig. 8A, oligo dT alone). These bands had migration patterns expected for full-length M2, sc4, and M1 mRNAs (the lower cluster), N mRNA (the middle band), and G mRNA (the upper band), as predicted from RNA sequence analysis and observed by hybridization analyses of mRNAs isolated from infected tissue with gene-specific probes following gel electrophoresis (Fig. 1 and data not shown). In agreement with the previous analysis (54), RNase H digestion with the N-specific oligonucleotide showed that the center band corresponded with the N mRNA, because this band disappeared and two new products appeared (Fig. 8A, panel N specific). Furthermore, RNase H digestions in the presence of the M2-, sc4-, or M1-specific oligonucleotide indicated that each of these mRNAs was a component of the most rapidly migrating band, since in each case the intensity of the band decreased upon digestion, concomitant with the appearance of cleavage products of the expected size (Fig. 8A, M2, sc4, and M1 specific). In addition, the largest of the three bands appears to be the G mRNA, since this band disappeared when digested in the presence of a G mRNA-complementary oligonucleotide (Fig. 8A, G specific). However, in this instance, specific G mRNA degradation products were not detected, presumably because the major digestion product comigrated with the N mRNA. From these results, we conclude that full-length, polyadenylated mRNAs for at least five of the six viral genes were synthesized during the course of this experiment.

TABLE 1. Quantification of SYNV transcription in vitro during sequential 1-h periods

	% N mRNA				
	0–1 h[b]	1–2 h	3–4 h	7–8 h	Avg[a]
M2	<10	88	55	41	61
sc4	<10	73	68	42	61
M1	<10	<10	45	20	33
G	<10	<10	23	13	18
L	<10	<10	12	ND[c]	12

[a] Calculated as the average percentage of the N mRNA (as a reference set at 100%), using all time points where >10% of the N mRNA was detected (three time points for the M2 and sc4 products, two for the M1 and G products, and one for the L gene product).
[b] Time of radiolabeling.
[c] ND, not determined.

The time course experiments also provided additional evidence for the sequential synthesis of SYNV mRNAs in vitro (Fig. 8). After 1 h, the primary product was the N mRNA. By 2 h, the M2 mRNA and smaller amounts of the sc4 mRNAs were also detected, while the M1 and G mRNAs accumulated to detectable levels only after 4 h of incubation. Although the experimental design precludes accurate quantification of the relative rates of accumulation, the overall trend observed is similar to that detected in the data presented in Fig. 7. Thus, sampling of both the 5′ ends to the polyadenylated full-length mRNA products indicates that mRNA synthesis occurs sequentially down the SYNV genomic template, beginning with the N gene.

In addition to the three predominant bands detected among the transcription products, a fourth band of lower intensity was also present (Fig. 8B). This RNA, which was larger than the 2-kb G mRNA, accumulated with kinetics similar to those of sc4 and M1, and it appeared before the G mRNA band. Interestingly, this species was digested by RNase H in the presence of oligonucleotides complementary to sequences within both the N and M2 mRNAs (Fig. 8B, N and M2 specific). In contrast, the RNA was insensitive to internal RNase H cleavage in the presence of the sc4, M1, and G oligonucleotides (Fig. 8B, sc4, M1, and G specific). Digestion with oligo (dT) also had no observable effect on the migration of this RNA

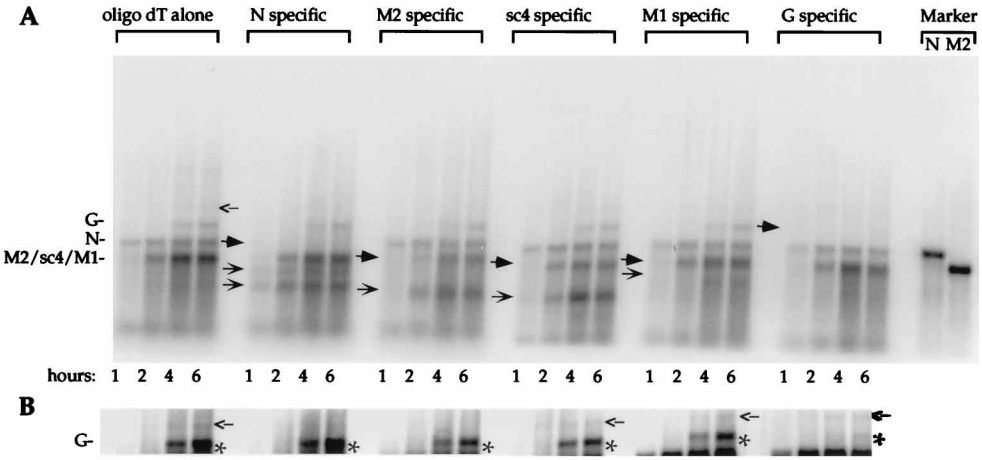

FIG. 8. RNase H analysis of polyadenylated RNA from in vitro SYNV polymerase reactions. RNAs from reaction mixtures containing radioactive UTP from time zero were terminated after 1, 2, 4, and 6 h of incubation and fractionated by oligo(dT)-cellulose chromatography. Aliquots of each bound fraction [poly(A)$^+$ RNAs] were then digested with RNase H in reaction mixtures containing oligo(dT) to increase the resolution of the products after hybridization. The reactions mixtures used for the panels contained, from left to right, only oligo(dT) or oligo(dT) plus DNA oligonucleotides complementary to SYNV N (oligoN2), M2 (oligoT2), sc4 (oligoS2), M1 (oligoO1), or G (oligoG2) mRNAs. (A) The full-length radiolabeled mRNA products (→) as well as specific cleavage products (➔) were visualized on a PhosphorImager following glyoxylation and agarose gel electrophoresis. Full-length transcripts of N and M2 mRNAs from cDNA clones are shown on the right as size markers. (B) A longer exposure of a portion of the gels shown in panel A reveals an additional minor RNA band (←), which is also visible in panel A, oligo(dT) alone. The G mRNA is identified with asterisks for reference. For this experiment, four replicate reactions were conducted under standard conditions except that 2 mM ATP, 1 mM CTP, 1 mM GTP, 100 mM unlabeled UTP, 100 μCi of [α-^{32}P]UTP, 5 mM phosphocreatine, and 2 U of phosphocreatine kinase were included in each reaction mixture. At the designated times, 50-μl aliquots were removed from each reaction mixture and pooled, and the RNA was extracted and selected on oligo(dT)-cellulose. Note that oligo(dT) was included in all RNase H digestions to increase the resolution of the products, particularly the cleavage products corresponding to the 3′ end of each gene.

species (Fig. 8B, oligo dT alone). Taken together, these results suggest that the product is derived from a direct read-through between the N and M2 genes. Similar read-through products have been detected both in VSV-infected cells and among the in vitro products of the VSV polymerase (21, 34). As with VSV, it is unclear whether the apparent SYNV read-through products are precursors to the monocistronic mRNAs or are aberrant replication attempts.

The in vitro-synthesized RNAs have messenger activity. To determine whether the transcribed RNAs could function as templates for translation, oligo(dT)-selected RNAs were purified after 6 h of synthesis in the polymerase extract. These RNAs were used to program a rabbit reticulocyte lysate in the presence of [^{35}S]methionine, and the radiolabeled polypeptide products were resolved by SDS-PAGE (Fig. 9, lane 3). To assist in identification of these products, proteins radiolabeled in infected protoplasts were immunoprecipitated by SYNV-specific antiserum and electrophoresed on the same gel (Fig. 9, lane 5). Comparison of these two lanes reveals that in the presence of oligo(dT)-selected RNAs, substantial quantities of translation products that comigrated with the N, M1, and M2 marker proteins accumulated. In a parallel translation of RNA purified from a 6-h reaction in extracts derived from uninfected tissue, polypeptides corresponding in size to the M2 and M1 proteins were not present, and only minor amounts of an unidentified polypeptide that had mobility similar to that of the N protein were detected (Fig. 9, lane 1). These results suggest that the major polypeptides detected were translated from SYNV mRNAs. However, SYNV mRNAs could have been present in the polymerase extract prior to in vitro transcription. To test this possibility, a transcription reaction was terminated immediately after adding the polymerase, and the recovered RNA products were used to program the rabbit reticulocyte lysate (Fig. 9, lane 2). Low levels of incorporation into polypeptides that comigrated with the SYNV polypeptides were observed, possibly suggesting that some full-length mRNAs were present in the polymerase extract. However, the marked stimulation of synthesis of the SYNV polypeptides in translation reaction mixtures containing RNAs resulting from the 6-h transcription reaction strongly suggests that full-length,

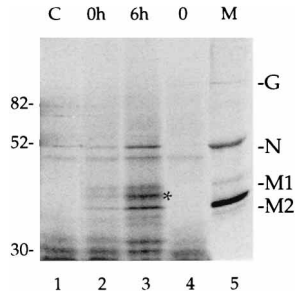

FIG. 9. In vitro translation of poly(A)$^+$ RNA synthesized in transcription reactions containing polymerase and control extracts. Unlabeled RNA was purified from the polymerase reaction mixtures containing 500 μM unlabeled UTP, and poly(A)$^+$ RNA was selected with oligo(dT)-cellulose. Lane 1 (C) shows translation products resulting from RNA recovered after transcription with control extracts from uninfected plants. Lane 2 (0h) shows the minor SYNV translation products resulting from endogenous SYNV mRNAs present in the polymerase extract. In this case, the endogenous RNAs were recovered from a transcription reaction that was terminated immediately after addition of the SYNV polymerase extract to the reaction. Lane 3 (6h) shows the more abundant SYNV translation products resulting from RNAs transcribed after a 6-h polymerase reaction. The in vitro translation reactions were programmed with one half of each poly(A)$^+$ sample (lanes 1 to 3) and then incubated for 1 h at 28°C in a rabbit reticulocyte lysate as specified by the supplier (4 μl of lysate in a 10-μl reaction mixture). Lane 4 (0) shows a parallel control translation experiment conducted without addition of RNA. After translation, 5 μl of each reaction was resolved by electrophoresis in SDS–10% polyacrylamide gels, and the radiolabeled polypeptide products were visualized on a PhosphorImager. The locations of radiolabeled size markers are shown on the left in kilodaltons, and the locations of SYNV proteins recovered after immunoprecipitation from infected protoplasts radiolabeled with [^{35}S]methionine (lane 5) are shown on the right. Note that the band identified by an asterisk in lane 3 may correspond to the sc4 translation product, as discussed in the text.

translationally active SYNV mRNAs were synthesized in vitro during the incubation period.

In addition to the translation products that comigrated with the N, M2, and M1 proteins, several unidentified polypeptides that were absent in the negative controls appeared after translation of the 6-h transcription products (Fig. 9; compare lane 3 with lanes 1 and 4). The largest and most prominent of these polypeptides (identified with an asterisk in Fig. 9, lane 3), migrated slightly more rapidly than the putative M1 product and probably corresponds to the sc4 protein. Interestingly, our previous analysis of the sc4 protein revealed that the protein migrated as a broad, heterogeneous band when isolated from cell extracts, but when it was isolated from virions, a single form that comigrated with M1 predominated, suggesting that the sc4 protein is posttranslationally modified prior to incorporation into virus particles (51, 55). The mobility of the unidentified species is appropriate for an unmodified or incompletely modified sc4 intermediate.

Two short genome-sense RNAs correspond to minus-strand leader RNAs. Previous size fractionation of the RNA synthesized in SYNV polymerase extracts revealed a population of short RNAs (<250 nt) that hybridized to a double-stranded DNA probe derived from a region corresponding to the 3′ end of the L gene and a small portion of the trailer region (nt 90 to 932 from the 5′ end of the genomic RNA; see Fig. 1 for location) (54). Given their small size, these products were unlikely to have been intermediates in L mRNA transcription. An alternative hypothesis was that the labeled RNAs correspond to the 5′ end of the genome-sense RNA and thus are distinct from the antigenomic mRNA products transcribed by the polymerase. To test this possibility, radiolabeled RNA products that had not been subjected to oligo(dT)-cellulose fractionation (total RNA products) were digested with RNase H in the presence of oligonucleotide probes complementary to the sequence located 160 to 176 bases from the 5′ end of the genomic RNA (Fig. 10, lane 4) or to the corresponding complementary antigenomic RNA sequence (Fig. 10, lane 2). As a control, the RNase H reactions were carried out without an added oligonucleotide (Fig. 10, lane 1). PAGE revealed that digestion in the presence of the genome-sense specific oligonucleotide resulted in cleavage of several products synthesized in vitro (Fig. 10; compare lane 4 with the products of digestion without an oligonucleotide in lane 1) as well as the appearance of a specific product of approximately 160 nt. The specificity of cleavage and the size of the cleavage product (ca. 160 nt) is consistent with that of a minus-sense RNA fragment corresponding to the 5′ end of the genomic RNA. Based on comparison with size markers, we estimate that the uncleaved species are approximately 200 and 230 nt in length, respectively. In contrast, we were unable to detect degradation of radiolabeled RNA species or the appearance of specific cleavage products following RNase H digestion in the presence of the oligonucleotide that is complementary to the positive-sense RNA (Fig. 10; compare lanes 1 and 2). This result suggests that the reaction mixtures contained very little, if any, discrete small products that were colinear with the 3′ end (trailer region) of the antigenome-sense RNA. Alternatively, the reaction mixtures could have contained small antigenome-sense RNA products that were colinear with the 3′ end of the L mRNA lacking a poly(A) tail. Such products would not have been detected by RNase H digestion in the presence of the probe located at the terminus of the L gene (Fig. 10, lane 2). Therefore, an RNase H digestion was also conducted after hybridization to an oligonucleotide predicted to cleave the L mRNA [lacking a poly(A) tail] ~160 nt from the 3′ end (Fig. 10, lane 3). However, this probe failed to generate a specific RNA cleavage product. Thus, the results indicate that the small RNAs detected previously (54) are colinear with the 3′ end of the genomic RNA, suggesting that replication was initiated but that extensive RNA elongation had not occurred. Therefore, during the in vitro reactions, minus-strand synthesis appears either to terminate and release truncated products or to pause at sites on the antigenome located at ca. 200 and 230 nt from the 3′ end.

DISCUSSION

Using polymerase activity partially purified from plant tissue, we have shown by several independent methods that the SYNV N, M2, and L proteins are associated with a transcriptionally active complex and that transcription of the viral genes conforms to a cascade pattern. This constitutes the first direct experimental evidence identifying the components of a viral polymerase from a plant-infecting rhabdovirus. The results underscore the conservation maintained within the rhabdovirus group despite a remarkable range of hosts infected. The likely homologs of the SYNV N, M2, and L proteins, namely, the VSV N, P, and L proteins and the rabies virus N, M1, and L proteins, respectively, are the viral proteins required for RNA synthesis in these pathogens (16, 25, 38, 39, 41, 42). The genomic location of each of these proteins is absolutely conserved, with the nucleocapsid protein gene being the first gene in each genome, the phosphoprotein the second, and the L protein the last. Given that the genome location is an important component of the regulation of gene expression in VSV and, likely SYNV (see below), this conservation of genome structure probably reflects requirements for high levels of nucleocapsid protein and low levels of L protein during the course of viral infection. The location of the M2 protein immediately following the N protein may reflect tandem, coordinated expression of these proteins, which, in the case of VSV, have been shown to interact (4).

Our results provide the most definitive evidence to date that the M2 protein is a VSV P protein homolog. Specifically, we have shown that the M2 protein, like the VSV P protein, is physically associated with the active polymerase complex. In contrast, we were unable to detect associations of the M1, G, or sc4 protein with this complex. Interestingly, we have also recently shown that the SYNV M2 protein is phosphorylated in vivo (55). Since the phosphorylation state of the VSV protein has been shown to be critical for the activity of the protein in transcription, these results suggest that the SYNV M2 protein exhibits both structural and functional conservation with the analogous phosphoproteins of related negative-strand RNA viruses that is not apparent from primary sequence comparisons.

The inhibition of SYNV polymerase activity by α-L antibodies suggests that the L protein has a direct role in SYNV RNA synthesis. Furthermore, the L protein is present in relatively low concentrations in the polymerase complex, suggesting that this protein may have a catalytic function. Multiple regions of homology between the SYNV and VSV L proteins, including the GDNQ motif which is absolutely conserved among the L proteins of the negative-strand RNA viruses sequenced to date (8), have been identified. It has been postulated that the GDNQ motif may be a component of the catalytic domain of the viral polymerase, as has been shown for a similar, highly conserved GDD motif found in the polymerases of positive-strand RNA viruses (31). Thus, our results provide direct biochemical evidence that the SYNV L protein is a viral polymerase component, confirming the predictions from the sequence analysis.

In addition to the active viral polymerase complex, we have

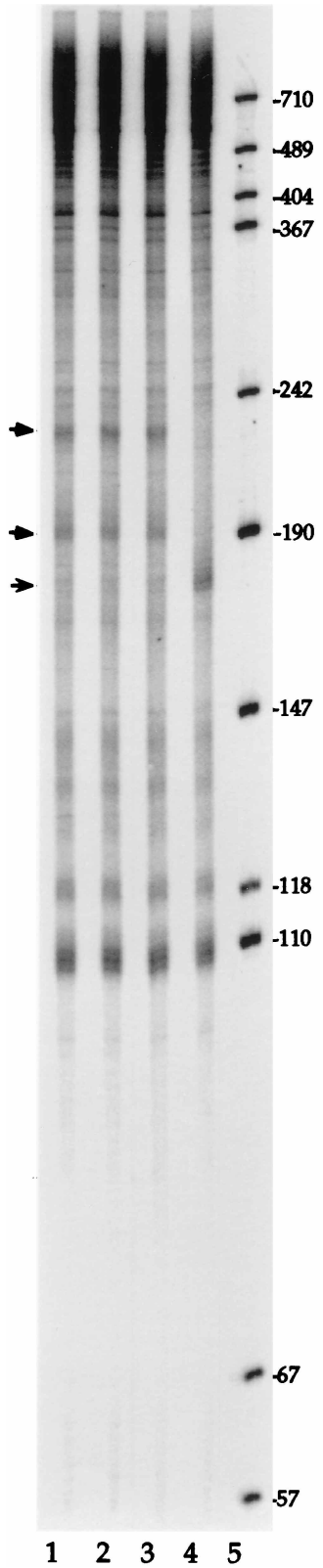

FIG. 10. Identification of putative minus-strand leader RNAs. Aliquots of RNA radiolabeled in a 30-min reaction were digested with RNase H lacking added oligonucleotides (lane 1) or after hybridization to messenger-sense specific oligonucleotide L3 (lane 2), messenger-sense specific oligonucleotide L2 (lane 3), or genome-sense specific oligonucleotide L3m (lane 4). RNAs were resolved by gel electrophoresis in a denaturing 6% polyacrylamide gel. The locations of two digestion-sensitive RNA species (→) and a specific cleavage product visible in lane 4 (➔) are shown on the left. Sizes of standards (lane 5) are indicated on the right in nucleotides.

identified a complex containing the L and M2 proteins. Complexes of the L and P proteins of Sendai virus, a paramyxovirus, are formed in cells which express these proteins in the absence of viral infection (24). Both Sendai virus proteins are required for defective interfering (DI) particle replication in vitro. Since mixtures of polypeptides expressed individually in separate cells prior to the in vitro replicase assay do not support DI replication, it was suggested that the Sendai virus L-P complexes were precursors to the viral polymerase. Thus, it is tempting to postulate that the SYNV L-M2 complex is also a precursor to the SYNV polymerase. This hypothesis will be tested in future experiments using the systems that we have developed.

Beyond the characterization of the SYNV polymerase components, the present study provides the first in-depth analysis of transcription by a nucleus-localized plant rhabdovirus polymerase. The expression of the SYNV genes in vitro is sequential because the mRNAs appeared temporally in the order of their location on the genome, beginning with the 3′-proximal N gene. A similar transcription pattern has previously been established for VSV, rabies virus, and a paramyxovirus, Sendai virus, based on the sensitivity of transcription to UV light exposure and in vitro transcription kinetics (1, 3, 17, 18, 26). We have also shown that SYNV transcription is discontinuous in vitro, because the steady-state levels of de novo-synthesized mRNAs displayed a cascade pattern whereby the N mRNA was produced most abundantly and each of the five other encoded mRNAs decreased progressively in abundance. Therefore, it is likely that SYNV gene expression is regulated at the level of transcription, as has been shown previously for the VSV gene products (26, 48, 53). The steady-state levels of SYNV proteins in infected cells have not been quantified, because accurate quantification is hampered by high levels of host protein translation, which is not diminished during SYNV infections (55). Thus, we are unable to state definitively that viral gene expression is primarily regulated at the transcription step. However, the low abundance of the L protein detected in extracts from infected plants and protoplasts (Fig. 3 and reference 54) certainly corresponds to the comparatively low levels of L mRNA transcription in vitro and L mRNA accumulation in vivo (Fig. 7 and 8 and references 29 and 47), suggesting that the accumulation of L protein is determined primarily by transcriptional regulation.

If the transcripts that we have detected were primarily due to run-on synthesis of nascent mRNAs initiated in vivo prior to polymerase extraction, one would have expected steady-state levels of transcription at early times in the reaction. However, in the in vitro system, the 3′-proximal genes were transcribed first, and the system required approximately 3 h to reach a steady-state level. This observation is most easily explained by the hypothesis that the in vivo transcription process is terminated during polymerase purification. We believe it is most likely that the nascent mRNAs are physically separated from the transcription complex during salt treatment or gradient centrifugation, as has been observed during centrifugation of VSV polymerase complexes over Renographin gradients (23). Alternatively, RNase degradation of the nascent mRNA during purification is also plausible since the mRNAs, unlike the genomic RNA, are probably not encapsidated and therefore could be more accessible to nucleases released during cell disruption.

Complete SYNV replication, or the synthesis of full-length genomic and antigenomic RNA, was not detected in vitro. Since it is likely that ongoing genome replication occurred in the infected tissue prior to polymerase purification, we believe that the isolation procedure depleted the nuclear extract of one or more factors required for replication. The N protein is

		I	II	III
Gene junction consensus		AUUCUUUUU/	GG	/UUG$^{UC}_{AA}$
Antigenome	13497-13482	AUAUUAUAA/	GG	/AAGUU
	13528-13513	UGUGUUAAA/	GG	/ACCUU

FIG. 11. Alignment of two putative modulation signals located on the SYNV antigenomic RNA (at positions 13497 to 13482 and 13528 to 13513) with the conserved gene junction sequence on the genomic RNA (20). Three conserved elements (I, II, and III) in the gene junction sequence on the genomic RNA are shown above the two putative modulation sequences. The conserved gene junction elements include the region encoding the 3′ end of the mRNA (I), the nontranscribed GG intergenic region (II), and the 5′ end of the subsequent gene (III). The 3′ end of each sequence is on the left. Note that termination or pausing of an RNA initiated from the 3′-terminal nucleotide of the antigenomic template at the first G residue of region II of the modulation signals would generate minus-sense RNAs of 200 and 231 nt.

a requisite factor for VSV replication (41). Hence, it is possible that depletion of N protein was responsible for the lack of RNA replication in the SYNV extract. Our results differ from those of others using VSV polymerase purified from infected tissue because replication was detected in the VSV systems (22, 43). The simplest hypothesis to explain this difference is that a soluble form of the N protein leached from the nuclei during purification and that the VSV systems used whole crude cytoplasmic extracts containing the requisite factors. Supplementing the nuclear extract with purified N protein or use of an in vitro transcription-translation system similar to that developed by Patton et al. for VSV (40) should enable testing of this hypothesis.

Even though we did not detect replication of full-length SYNV genomic RNA in the polymerase extract, we have identified two discrete minus-sense RNA products that appear to be initiated at the 3′ end of the antigenomic RNA template and are thus colinear with the 5′ end of the genomic RNA. These two small genome-sense RNA species were not bound by oligo(dT)-cellulose (54), suggesting that they are not polyadenylated. The accumulation of these RNAs may indicate that regulatory or modulation sites directing preferential attenuation of replication are present on the antigenomic template and that these modulation sites are operational in the in vitro system. According to this model, initiation of genomic RNA synthesis occurred in vitro, but RNA elongation was constrained at two specific sites. The nascent RNAs were released either when the polymerase complex encountered the modulation signals or, alternatively, during RNA extraction. Leppert et al. have also identified short RNAs that are colinear with the 5′ end of VSV genomic RNA, which they have designated minus-strand leader RNAs (32). These RNAs are detected in VSV-infected cells but are particularly abundant in the presence of DI particles. Leppert et al. (32) have suggested that these RNAs are the result of premature termination of genomic RNA synthesis that occurs when the concentrations of N protein fall below those needed for encapsidation of the nascent replicating RNA, in a fashion analogous to intergenic termination of antigenome synthesis (2). Premature termination or pausing of genomic sense replication, then, would be particularly frequent in the presence of DI RNAs, which would constitute a sink for available N protein.

Specific sites on the genomic RNA of rhabdoviruses where regulated attenuation of viral replication occurs (as well as termination of viral transcription), namely, the gene junction sequences (20, 49), have been known for quite some time. The discrete sizes of the two predominant genomic sense SYNV RNA products (ca. 200 and 230 nt), therefore, prompted us to examine the sequence at these locations on the antigenome (Fig. 11). Interestingly, the examination revealed regions that have attributes in common with the gene junction sequences of the genomic RNA (20). The SYNV gene junction sequences are composed of three conserved sequence elements: a poly(U) tract at the 5′ end of each gene on the genomic template (element I), a nontranscribed GG dinucleotide (element II), and a sequence located at the beginning of the subsequent gene (element III) (for discussions see references 4 and 20). The exact element I sequence may be required as a signal for polyadenylation, as suggested by the analysis of the SYNV leader-N junction (54), while element III may be a component of the mRNA promoter. The putative modulation signals present near the 3′ end of the antigenomic RNA each contain a GG dinucleotide, the invariant element II of the gene junction sequences located on the genomic RNA (20). This dinucleotide is preceded by a poly(U/A) stretch that resembles but is not identical to the conserved element I. Element III is not conserved in these putative modulation signals. We propose that the dinucleotide GG, preceded by the poly(A/U) sequence, is a component of degenerate gene junction sequences that lack signals for polyadenylation or initiation of synthesis of internal RNAs but contain information sufficient for regulated attenuation of RNA replication.

Our observations are consistent with the model of Leppert et al. (32) and extend previous results in two important ways. First, the SYNV system is the only one where the putative minus-strand leader RNAs are easily detectable in the absence of DI RNAs. The SYNV system differs from the VSV virion- and cell-derived transcription-replication systems in that the SYNV antigenomic RNAs are easily detectable under conditions where replication is severely inhibited. Second, we suggest a mechanism underlying premature termination or pausing on an antigenomic template. Indeed, a particularly attractive feature of the model is that it posits that replication of both genomic and antigenomic intermediates is regulated by a common mechanism employing versions of the same *cis*-acting sequence elements. Obviously, the critical assumption underlying this analysis is that the short genome-sense RNAs represent authentic intermediates in the replication of full-length genomes. This assumption can be tested by fortification of our system with external factors, in particular the N protein as discussed above. Thus, the reconstitution of full-length replication with the polymerase extract is an important aspect of future research using this system.

In summary, VSV and SYNV have evolved substantially to accommodate their diverse hosts and different sites of replication (58), yet the overall similarity between SYNV transcription and that of VSV provides compelling evidence suggesting that the basic mechanisms regulating mRNA synthesis and genome replication are highly conserved features of rhabdovirus multiplication.

ACKNOWLEDGMENTS

We thank David Hacker, Caroline Kane, Diane Lawrence, Doris Wagner, and Huan Zhou for helpful discussions while this work was in progress. We also thank Diane Lawrence, Doris Wagner, and Ailsa Webster for reading the manuscript critically and Diane Lawrence for assistance with the figure graphics.

This research was supported by grants DMB 90-47486 and DMB 94-18086 from the National Science Foundation to A.O.J.

REFERENCES

1. **Abraham, G., and A. K. Banerjee.** 1976. Sequential transcription of the genes of vesicular stomatitis virus. Proc. Natl. Acad. Sci. USA **73:**1504–1508.
2. **Arnheiter, H., N. L. Davis, G. Wertz, M. Schubert, and R. A. Lazzarini.** 1985. Role of the nucleocapsid protein in regulating vesicular stomatitis virus RNA synthesis. Cell **41:**259–267.

3. **Ball, L. A., and C. N. White.** 1976. Order of transcription of genes of vesicular stomatitis virus. Proc. Natl. Acad. Sci. USA **73:**442–446.
4. **Banerjee, A. K.** 1987. Transcription and replication of rhabdoviruses. Microbiol. Rev. **51:**66–87.
5. **Banerjee, A. K., and S. Barik.** 1992. Gene expression of vesicular stomatitis virus genome RNA. Virology **188:**417–428.
6. **Blumberg, B. M., M. Leppert, and D. Kolakofsky.** 1981. Interaction of VSV leader RNA and nucleocapsid protein may control VSV genome replication. Cell **23:**837–845.
7. **Bras, F., D. Teninges, and S. Dezelee.** 1994. Sequences of the N and M genes of the sigma virus of Drosophila and evolutionary comparison. Virology **200:**189–199.
8. **Choi, T.-J., S. Kuwata, E. V. Koonin, L. A. Heaton, and A. O. Jackson.** 1992. Structure of the L (polymerase) protein gene of sonchus yellow net virus. Virology **189:**31–39.
9. **Christie, S. R., R. G. Christie, and J. R. Edwardson.** 1974. Transmission of a bacilliform virus of sowthistle and *Bidens pilosa*. Phytopathology **64:**840–845.
10. **Conzelmann, K. K.** 1996. Genetic manipulation of non-segmented negative-strand RNA viruses. J. Gen. Virol. **77:**381–389.
11. **Conzelmann, K. K., and M. Schnell.** 1994. Rescue of synthetic genomic RNA analogs of rabies virus by plasmid-encoded proteins. J. Virol. **68:**713–719.
12. **De, B. P., and A. K. Banerjee.** 1985. Requirements and functions of vesicular stomatitis virus L and NS proteins in the transcription process in vitro. Biochem. Biophys. Res. Commun. **126:**40–49.
13. **De, B. P., and A. K. Banerjee.** 1984. Specific interactions of vesicular stomatitis virus L and NS proteins with heterologous genome ribonucleoprotein template lead to mRNA synthesis in vitro. J. Virol. **51:**628–634.
14. **Emerson, S. U.** 1987. Transcription of vesicular stomatitis virus, p. 245–270. *In* R. R. Wagner (ed.), The rhabdoviruses. Plenum Press, New York, N.Y.
15. **Emerson, S. U., and R. R. Wagner.** 1973. L protein requirement for in vitro RNA synthesis by vesicular stomatitis virus. J. Virol. **12:**1325–1335.
16. **Emerson, S. U., and Y. Yu.** 1975. Both NS and L proteins are required for in vitro RNA synthesis by vesicular stomatitis virus. J. Virol. **15:**1348–1356.
17. **Flamand, A., and J. F. Delagneau.** 1978. Transcriptional mapping of rabies virus in vivo. J. Virol. **28:**518–523.
18. **Glazier, K., R. Raghow, and D. W. Kingsbury.** 1977. Regulation of Sendai virus transcription: evidence for a single promoter in vivo. J. Virol. **21:**863–871.
19. **Harlow, E., and D. Lane.** 1988. Antibodies: a laboratory manual. Cold Spring Harbor Laboratory Press, Cold Spring Harbor, N.Y.
20. **Heaton, L. A., B. I. Hillman, B. G. Hunter, D. Zuidema, and A. O. Jackson.** 1989. Physical map of the genome of sonchus yellow net virus, a plant rhabdovirus with six genes and conserved gene junction sequences. Proc. Natl. Acad. Sci. USA **86:**8665–8668.
21. **Herman, R. C., M. Schubert, J. D. Keene, and R. A. Lazzarini.** 1980. Polycistronic vesicular stomatitis virus RNA transcripts. Proc. Natl. Acad. Sci. USA **77:**4662–4665.
22. **Hill, V. M., L. Marnell, and D. F. Summers.** 1981. In vitro replication and assembly of vesicular stomatitis virus nucleocapsids. Virology **113:**109–118.
23. **Hill, V. M., C. C. Simonsen, and D. F. Summers.** 1979. Characterization of vesicular stomatitis virus replicating complexes isolated in renografin gradients. Virology **99:**75–83.
24. **Horikami, S. M., J. Curran, D. Kolakofsky, and S. A. Moyer.** 1992. Complexes of Sendai virus NP-P and P-L proteins are required for defective interfering particle genome replication in vitro. J. Virol. **66:**4901–4908.
25. **Howard, M., and G. Wertz.** 1989. Vesicular stomatitis virus RNA replication: a role for the NS protein. J. Gen. Virol. **70:**2683–2694.
26. **Iverson, L. E., and J. K. Rose.** 1981. Localized attenuation and discontinuous synthesis during vesicular stomatitis virus transcription. Cell **23:**477–484.
27. **Jackson, A. O.** 1987. Biology, structure, and replication of plant rhabdoviruses, p. 427–508. *In* R. R. Wagner (ed.), The rhabdoviruses. Plenum Press, New York, N.Y.
28. **Jackson, A. O.** 1978. Partial characterization of the structural proteins of sonchus yellow net virus. Virology **87:**172–181.
29. **Jones, R. W., and A. O. Jackson.** 1990. Replication of sonchus yellow net virus in infected protoplasts. Virology **179:**815–820.
30. **Konforti, B. B., M. J. Kozoilkiewicz, and M. M. Konarska.** 1993. Disruption of base pairing between the 5′ splice site and the 5′ end of U1 snRNA is required for spliceosome assembly. Cell **75:**863–873.
31. **Koonin, E. V., and V. V. Dolja.** 1993. Evolution and taxonomy of positive-strand RNA viruses: implications of comparative analysis of amino acid sequences. Crit. Rev. Biochem. Mol. Biol. **28:**375–430. (Erratum, **28:**546.)
32. **Leppert, M., L. Rittenhouse, J. Perrault, D. F. Summers, and D. Kolakofsky.** 1979. Plus and minus strand leader RNAs in negative strand virus-infected cells. Cell **18:**735–747.
33. **Masters, P. S., and A. K. Banerjee.** 1988. Complex formation with vesicular stomatitis virus phosphoprotein NS prevents binding of nucleocapsid protein N to nonspecific RNA. J. Virol. **62:**2658–2664.
34. **Masters, P. S., and C. E. Samuel.** 1984. Detection of in vivo synthesis of polycistronic mRNAs of vesicular stomatitis virus. Virology **134:**277–286.
35. **Milner, J. J., M. J. J. Hakkaart, and A. O. Jackson.** 1979. Subcellular distribution of RNA sequences complementary to sonchus yellow net virus RNA. Virology **98:**497–501.
36. **Milner, J. J., and A. O. Jackson.** 1979. Sequence complementarity of sonchus yellow net virus RNA with RNA isolated from the polysomes of infected tobacco. Virology **97:**90–99.
37. **Ongradi, J., C. Cunningham, and J. F. Szilagyi.** 1985. The role of polypeptides L and NS in the transcription process of vesicular stomatitis virus New Jersey using the temperature-sensitive mutant tsE1. J. Gen. Virol. **66:**1011–1023.
38. **Pattnaik, A. K., and G. W. Wertz.** 1991. Cells that express all five proteins of vesicular stomatitis virus from cloned cDNAs support replication, assembly, and budding of defective interfering particles. Proc. Natl. Acad. Sci. USA **88:**1379–1383.
39. **Pattnaik, A. K., and G. W. Wertz.** 1990. Replication and amplification of defective interfering particle RNAs of vesicular stomatitis virus in cells expressing viral proteins from vectors containing cloned cDNAs. J. Virol. **64:**2948–2957.
40. **Patton, J. T., N. L. Davis, and G. W. Wertz.** 1983. Cell-free synthesis and assembly of vesicular stomatitis virus nucleocapsids. J. Virol. **45:**155–164.
41. **Patton, J. T., N. L. Davis, and G. W. Wertz.** 1984. N protein alone satisfies the requirement for protein synthesis during RNA replication of vesicular stomatitis virus. J. Virol. **49:**303–309.
42. **Peluso, R. W.** 1988. Kinetic, quantitative, and functional analysis of multiple forms of the vesicular stomatitis virus nucleocapsid protein in infected cells. J. Virol. **62:**2799–2807.
43. **Peluso, R. W., and S. A. Moyer.** 1983. Initiation and replication of vesicular stomatitis virus genome RNA in a cell-free system. Proc. Natl. Acad. Sci. USA **80:**3198–3202.
44. **Peluso, R. W., and S. A. Moyer.** 1988. Viral proteins required for the in vitro replication of vesicular stomatitis virus defective interfering particle genome RNA. Virology **162:**369–376.
45. **Pennica, D., K. R. Lynch, P. S. Cohen, and H. L. Ennis.** 1979. Decay of vesicular stomatitis virus mRNAs in vivo. Virology **94:**484–487.
46. **Perrault, J., G. M. Clinton, and M. A. McClure.** 1983. RNP template of vesicular stomatitis virus regulates transcription and replication functions. Cell. **35:**175–185.
47. **Rezaian, M. A., L. A. Heaton, K. Pederson, J. J. Milner, and A. O. Jackson.** 1983. Size and complexity of polyadenylated RNAs induced in tobacco infected with sonchus yellow net virus. Virology **131:**221–229.
48. **Rhodes, D. P., S. A. Moyer, and A. K. Banerjee.** 1974. In vitro synthesis of methylated messenger RNA by the virion-associated RNA polymerase of vesicular stomatitis virus. Cell **3:***327–333.*
49. **Rose, J. K.** 1980. Complete intergenic and flanking gene sequences from the genome of vesicular stomatitis virus. Cell **19:**415–421.
50. **Schneemann, A., P. A. Schneider, R. A. Lamb, and W. I. Lipkin.** 1995. The remarkable coding strategy of Borna disease virus: a new member of the nonsegmented negative strand RNA viruses. Virology **210:**1–8.
51. **Scholthof, K. B., B. I. Hillman, B. Modrell, L. A. Heaton, and A. O. Jackson.** 1994. Characterization and detection of sc4: a sixth gene encoded by sonchus yellow net virus. Virology **204:**279–288.
52. **Tordo, N., P. De Haan, R. Goldbach, and O. Poch.** 1992. Evolution of negative-stranded RNA genomes. Semin. Virol. **3:**341–357.
53. **Villarreal, L. P., M. Breindl, and J. J. Holland.** 1976. Determination of molar ratios of vesicular stomatitis virus induced RNA species in BHK21 cells. Biochemistry **15:**1663–1667.
54. **Wagner, J. D. O., T. J. Choi, and A. O. Jackson.** 1996. Extraction of nuclei from sonchus yellow net rhabdovirus-infected plants yields a polymerase that synthesizes viral mRNAs and polyadenylated plus-strand leader RNA. J. Virol. **70:**468–477.
55. **Wagner, J. D. O., and A. O. Jackson.** Unpublished observations.
56. **Wagner, R. R.** 1990. Rhabdoviridae and their replication, p. 867–881. *In* B. N. Fields and D. M. Knipe (ed.), Virology, 2nd ed, vol. 1. Raven Press, New York, N.Y.
57. **Wagner, R. R.** 1987. Rhabdovirus biology and infection: an overview, p. 9–74. *In* R. R. Wagner (ed.), The rhabdoviruses. Plenum Press, New York, N.Y.
58. **Wetzel, T., R. G. Dietzgen, and J. L. Dale.** 1994. Genomic organization of lettuce necrotic yellow rhabdovirus. Virology **200:**401–412.
59. **Wunner, W. H., C. H. Calisher, R. G. Dietzgen, A. O. Jackson, E. W. Kitajima, M. Lafron, J. M. Leong, S. Nichols, J. S. Smith, and P. J. Walker.** 1995. Family Rhabdoviridae, p. 275–288. *In* F. A. Murphy, C. M. Fauquet, D. H. L. Bishop, S. A. Ghabriel, A. W. Jarvis, G. P. Martelli, M. A. Mayo, M. D. Summers (ed.), Virus taxonomy: classification and nomenclature of viruses: sixth report of the International Committee on Taxonomy of Viruses. Springer-Verlag, Vienna, Austria.